PACS: 73.61.Ey, 61.10.Nz, 61.72.Dd, 81.40.Vw

J. Bak-Misiuk[1], P. Romanowski[1], J. Domagala[1], A. Misiuk[2], E. Dynowska[1], E. Lusakowska[1], A. Barcz[1], J. Sadowski[1,3], W. Caliebe[4]

FERROMAGNETIC NANOCLUSTERS IN Si:Mn AND GaMnAs ANNEALED AT HIGH TEMPERATURE–PRESSURE

[1]Institute of Physics, Polish Academy of Sciences
Al. Lotnikow 32/46, 02-668 Warsaw, Poland
E-mail: bakmi@ifpan.edu.pl

[2]Institute of Electron Technology
Al. Lotnikow 46, 02-668 Warsaw, Poland

[3]Lund University, MAX-Lab
Lund, SE-221 00, Sweden

[4]Hasylab Desy
Notkerstrasse 85, D-22603 Hamburg, Germany

We report the results of defect structures studies of silicon implanted at different temperatures with Mn ions (Si:Mn) and of GaMnAs layers, next annealed under ambient and high pressures. An influence of annealing conditions on structural properties of Si:Mn and GaMnAs layers was investigated. It has been confirmed that annealing of the Si:Mn samples after implantation results in crystallization of silicon inside the buried post-implanted layer, as well as in the formation of ferromagnetic Mn_4Si_7 precipitates. A change of strain in the GaMnAs layer, from the compressive to the tensile one, related to a creation of nanoclustered MnAs, was found to be dependent on processing conditions and primary existing structural defects, while independent of the Mn concentration. An influence of primary defects on the structural transformations of the GaMnAs layer is discussed.

1. Introduction

Ferromagnetic semiconductors have recently received much interest, since they hold out prospects for using electron spins in electronic devices. Ion implantation has been utilized to achieve ferromagnetism in semiconductor crystals. Ferromagnetic ordering in Si implanted with Mn^+ ions (Si:Mn) has been reported recently; this ordering is evidently related to the structure of Mn-enriched near-surface layer in the implanted material. It has been found that, for Si:Mn produced by implantation with Mn^+ doses, $D = 10^{15}$–10^{16} cm^{-2}, at energy, E = 300 keV, Curie temperature exceeds 400 K after rapid thermal annealing at 1070 K [1]. Ferromagnetic properties of Si:Mn have been attributed to the formation of $MnSi_{1.7}$ [2].

Among the compounds that can be used in spintronics, those created by introducing ferromagnetic inclusions into the semiconducting matrix seem to be especially promising. In order to obtain materials with desired magnetic properties, it is reasonable to start with inclusions with Curie temperature, T_C, above the room one. The granular GaAs:MnAs material is a possible candidate because it exhibits ferromagnetic/superparamagnetic behavior at room temperature, dependent on MnAs cluster size [3–6].

As it has been stated, not only temperature but also enhanced hydrostatic pressure (*HP*) at processing of Si:Mn affect its magnetic properties [7].

This paper is focused on investigation of the defect structure of Si:Mn and GaMnAs annealed under ambient and enhanced hydrostatic pressures.

2. Experimental

Cz–Si with oxygen concentration $9 \cdot 10^{17}$ cm^{-3} or Fz–Si were implanted with 160 keV Mn^+ ions at substrate temperature (T_s) 340 or 610 K, to a dose, $D = 1 \cdot 10^{16}$ cm^{-2}. Si:Mn was processed for 1 h at up to 1270 K under ambient or enhanced hydrostatic pressures, up to *HP* = 1.1 GPa. Structural characterization of the samples, before and after processing, was performed using synchrotron radiation at the W1.1 beamline of Hasylab-Desy.

GaMnAs/GaAs samples were also studied. GaMnAs layers were grown on the 001 oriented GaAs substrates by MBE (Molecular Beam Epitaxy). After growth the GaMnAs/GaAs samples were processed for 1 h at *HT* = 650 K under ambient pressure (10^5 Pa) and *HP* = 1.1 GPa in Ar atmosphere. The samples processed for 1 h at *HT* = 650 K under 10^5 Pa were subsequently treated for 1 h at 920 K under *HP* = 1.1 GPa.

We investigated an influence of the *HP–HT* treatment on the defect structure for two kinds of GaMnAs/GaAs samples with the same thickness (0.8 μm) of the GaMnAs layer:

I – with the out-of-plane lattice parameter of GaMnAs **higher** than that of the substrate, after annealing at 670 K under 10^5 Pa (samples Ia and Ib, Table);

II – with the out-of-plane lattice parameter of GaMnAs **lower** (due to a creation of nanoclusters) than that of the substrate after annealing at 670 K under 10^5 Pa (sample II, Table).

Table

Out-of-plane lattice parameters ($a_{\text{as-grown}}$, a_T, a_{HP-T}) and in-plane strain, before ($\varepsilon_{\text{as-grown}}$) and after annealing under 10^5 Pa (ε_T) and under *HP* (ε_{HP-T}); 670 K–1.1 GPa

Sample	Mn content, %	$a_{\text{as-grown}}$	a_T	a_{HP-T}	$\varepsilon_{\text{as-grown}}$	ε_T	ε_{HP-T}
		Å			$\times 10^{-4}$		
Ia	1.0	5.6592	5.6568	5.6574	–5.66	–3.54	–4.24
Ib	5.5	5.6806	5.6538	5.6542	–24	–0.71	–0.84
II	2.0	5.6607	5.6525	5.6511	–6.71	0.17	0.35

The defect structure of GaMnAs/GaAs was determined by high resolution X-ray diffraction method. The lattice parameters for GaMnAs, before and after *HP–HT* processing, were determined to an accuracy of 10^{-4} Å. Reciprocal space maps were registered for the (004) symmetrical reflections.

Atomic Force Microscopy measurements (AFM) were performed with Digital Instrument in the tapping mode; the root mean square (RMS) roughness was determined (RMS is defined as a standard deviation of the roughness in the direction perpendicular to the surface).

3. Results and discussion

For Cz–Si:Mn implanted at T_s = 340 K with D =1·10^{16} cm^{-2} (Fig. 1), the buried implanted layers are amorphous, both just after implantation and after processing at 610 K. The reflections from polycrystalline Si were detected after the treatment at 870 K, showing on re-crystallization of nanocrystalline layer (Fig. 1). Also peaks of small intensity corresponding to the ferromagnetic Mn_4Si_7 phase were observed. No influence of hydrostatic pressure applied during annealing on the defect structure of Si:Mn was detected for these samples.

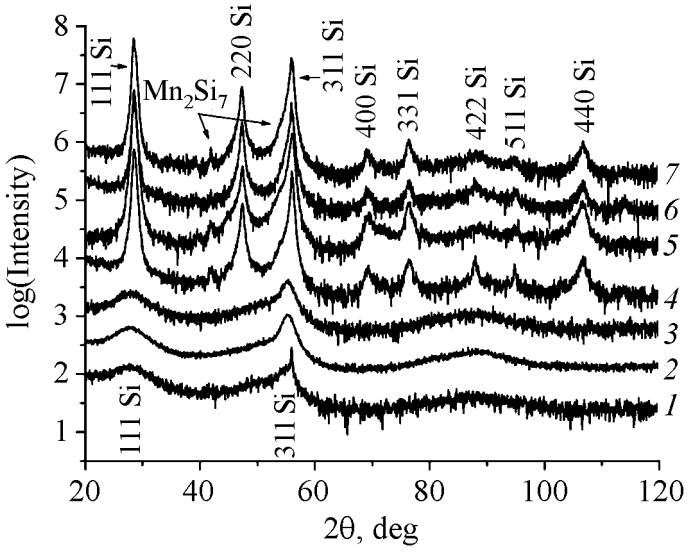

Fig. 1. Coplanar 2θ scan in grazing incidence geometry for Cz-Si:Mn implanted (D = = 1·10^{16} cm^{-2}) at 340 K: *1* – as-implanted; *2*, *4*, *6* – annealed at 610, 870, and 1070 K, respectively, under 10^5 Pa; *3*, *5*, *7* – processed for 1 h at 610, 870, and 1070 K, respectively, under 1.1 GPa

In the case of Fz–Si implantation at T_s = 610 K, the reflections coming from polycrystalline Si are detected. The reflections from the Mn_4Si_7 phase are visible after annealing at 870 K (Fig. 2). An increase of processing temperature up to 1070 K results in the increased intensity of reflection originating from the presence of the Mn_4Si_7 phase. *HP* applied during processing influences re-crystallization of implantation – damaged material as results from observation of reflections from the polycrystalline Si fraction (Fig. 2). Simultaneously, annealing at 1070 K under *HP* results in the increased peak intensity coming from the ferromagnetic Mn_4Si_7 phase (compare Fig. 2, curves *6* and *7*).

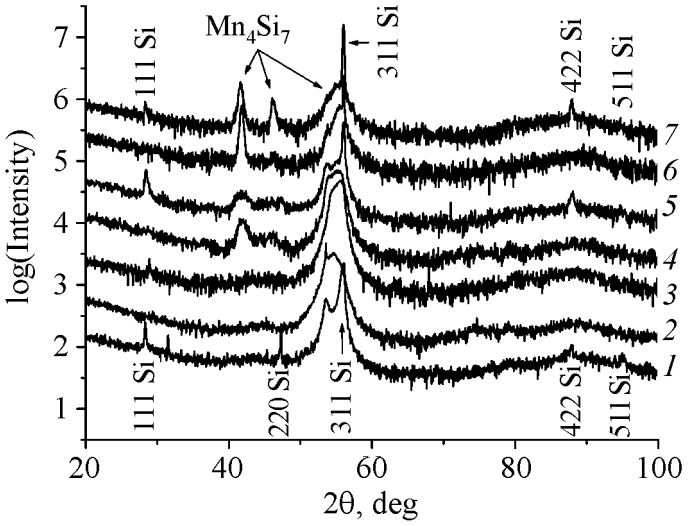

Fig. 2. Coplanar 2θ scan in grazing incidence geometry for Fz-Si:Mn implanted (D = $= 1 \cdot 10^{16}$ cm^{-2}) at 610 K: *1* – as-implanted; *2*, *4*, *6* – annealed at 610, 870, and 1070 K, respectively, under 10^5 Pa; *3*, *5*, *7* – processed for 1 h at 610, 870, and 1070 K, respectively, under 1.1 GPa

The X-ray 2θ/ω scans (004 reflection) for the GaMnAs layers, as-grown and treated at 670 K–10^5 Pa and at 670 K–1.1 GPa, are presented in Fig. 3 for the mentioned two kinds of samples. From the diffraction peak positions, the out-of-plane parameters of the layer material and in-plane strain, ε (ε = $a_{II} - a_{relax}/a_{relax}$, where: a_{relax} and a_{II} are, respectively, the relaxed and in-plane lattice parameters of the layer material) were calculated.

The out-of-plane lattice parameters measured to an accuracy of 10^{-4} Å and the strain values are listed in Table.

In the case of Ia and Ib samples, a decrease of the out-of-plane lattice parameter value is distinctly more pronounced for the *HT*-processed samples in comparison to those treated at *HP–HT* (Fig. 3 and Table) while still remains higher than the lattice parameter of GaAs (5.6533 Å). Before and after processing, the layers remained to be under compressive strain. More pronounced decrease of the lattice parameter of the Ia and Ib type GaMnAs layers after processing under ambient pressure (10^5 Pa), in comparison to that after processing under *HP*, can be explained by decreased diffusivity of Mn interstitials in GaMnAs under *HP*. It has been reported earlier that *HP* can modify substantially diffusivity of dopants [9]. An influence of the *HP*-related changes on a concentration of As antisites and on a creation of As clusters can influence the lattice parameter value as well.

In the case of processed II type sample, the out-of-plane and relaxed lattice parameters are lower than those of GaAs. This means that GaMnAs is under tensile stress. This effect is even more marked for the *HP–HT* treated sample (Fig. 3,*b*, Table). A change of strain, from the compressive to tensile state, has been reported to be related to a creation of MnAs nanoclusters [3–6]. During the *HP–HT* treatment, different compressibility of the MnAs nanoclusters and of the GaAs matrix involves a volume mismatch and additional internal strain is built up resulting in observed decrease of the lattice parameters of the GaAs matrix.

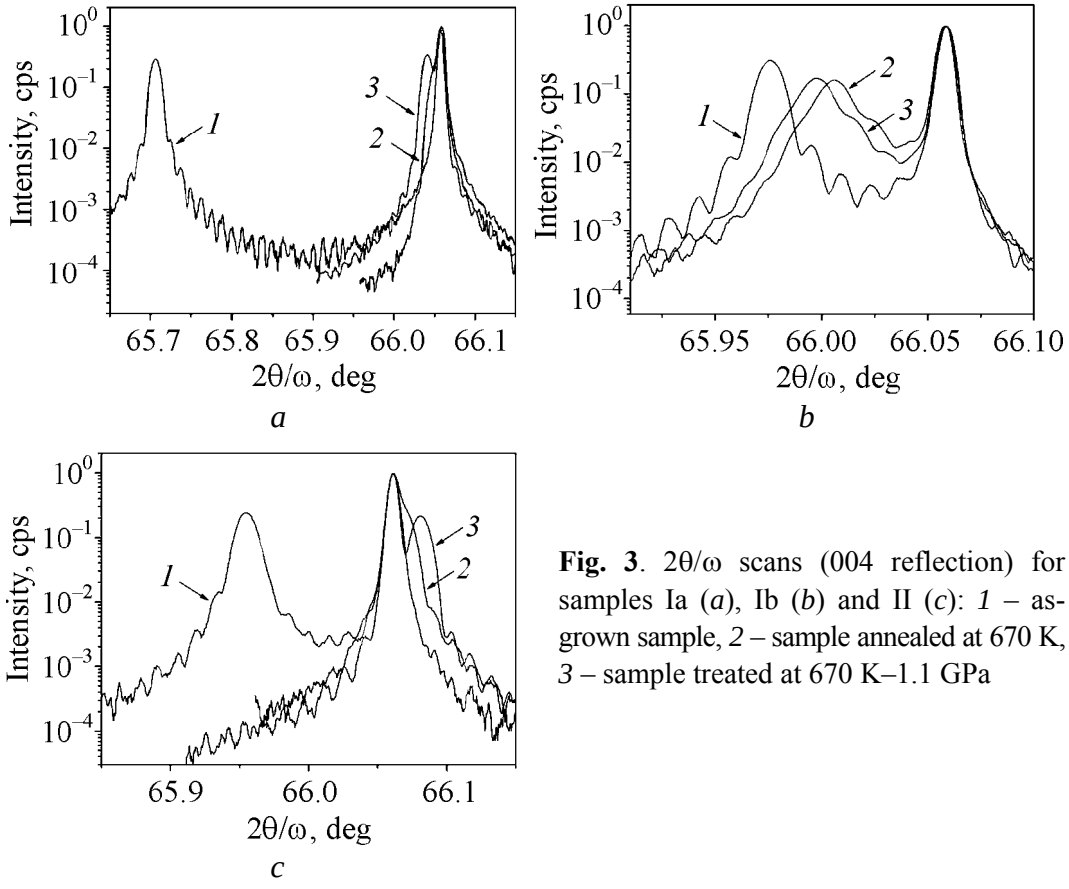

Fig. 3. 2θ/ω scans (004 reflection) for samples Ia (*a*), Ib (*b*) and II (*c*): *1* – as-grown sample, *2* – sample annealed at 670 K, *3* – sample treated at 670 K–1.1 GPa

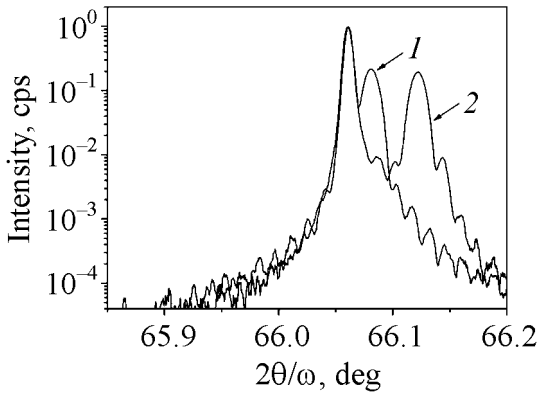

Fig. 4. Comparison of 2θ/ω scans (004 reflection) for sample II treated at: *1* – 670 K–1.1 GPa, *2* – 670 K–10^5 Pa + 920 K–1.1 GPa

An influence of temperature applied during the *HP–HT* treatment on the structure of sample II is presented in Fig. 4. The diffraction peaks for GaMnAs after processing at 920 K under 1.1 GPa are presented and compared with the diffraction peaks of GaMnAs after the treatment at 670 K–1.1 GPa. In the case of samples I processed at 920 K, polycrystallization of the layer material has been observed. In the case of sample II, the GaMnAs layer remains to be still single crystalline; its lattice parameters decrease in comparison to the case of sample treated at 670 K and strain, ε_{HP-T}, achieves the value equal to $4.07 \cdot 10^{-4}$. Structural changes after processing at various temperatures in the GaMnAs/GaAs samples are well visible on the reciprocal space maps (Fig. 5). More marked increase of diffuse scattering in the case of sample II in comparison to that in the Ia one, after annealing at 670 K under ambient (compare Fig. 5,*b*,*f*) and enhanced pressures (Fig. 5,*c*,*g*) are correlated

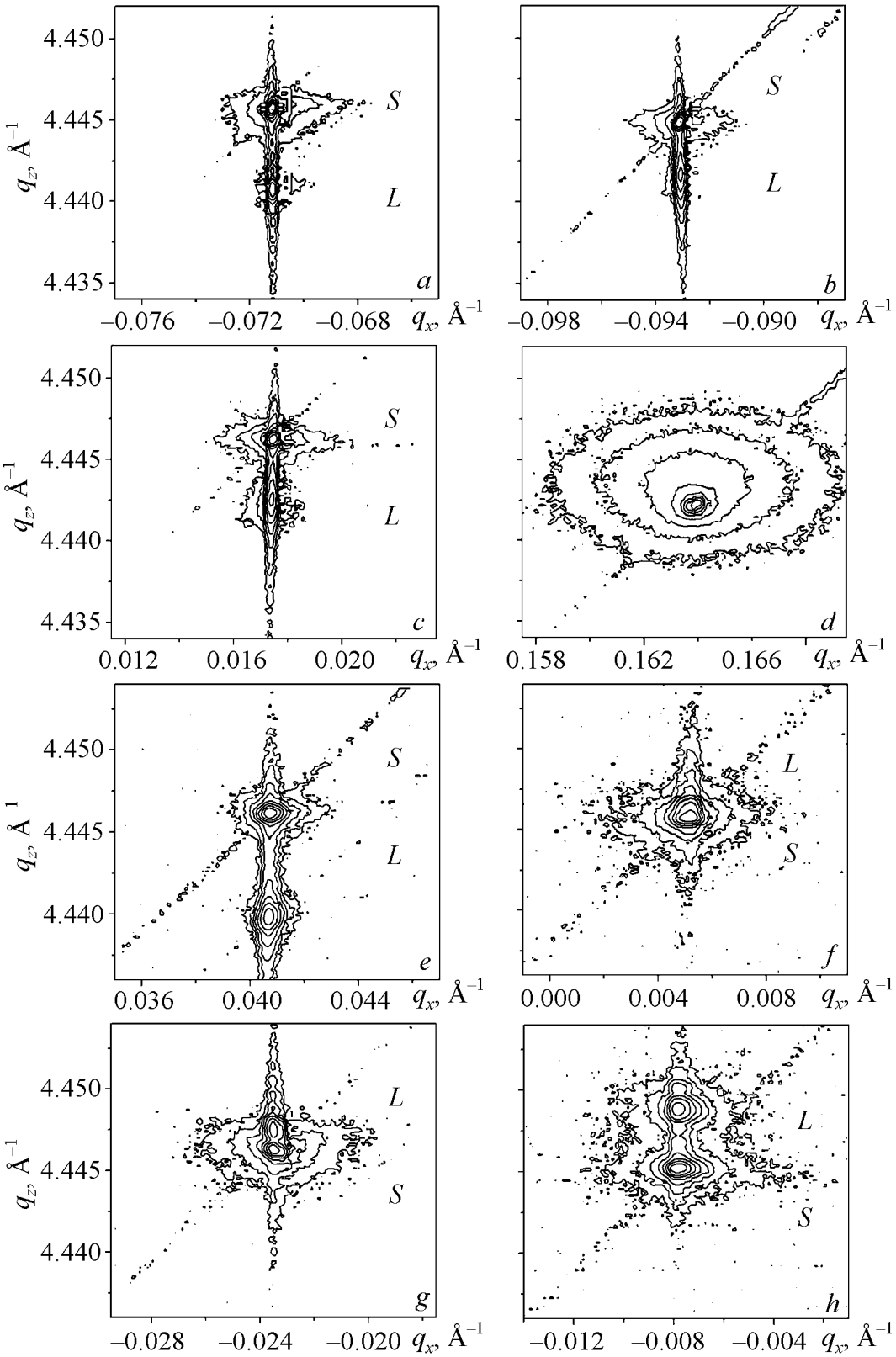

Fig. 5. 004 Reciprocal space maps of sample Ia (*a*, *b*, *c*, *d*) and of sample II (*e*, *f*, *g*, *h*): *a*, *e* – as-grown; *b*, *f* – annealed at *HT* = 650 K–10^5 Pa; *c*, *g* – treated at *HT* = 650 K–1.1 GPa; *d*, *h* – treated at 670 K–10^5 Pa + 920 K–1.1 GPa

with a formation of the granular structure in the sample II. It means that a creation of the granular structure in GaAs (containing MnAs nanoclusters) is accompanied with the formation of small clusters producing a large distortion of host lattice resulting, in turn, in increased diffuse scattering. No influence of high pressure on diffuse scattering and defect creation was found for the both sample kinds.

An increase of annealing temperature up to 920 K during the *HP–HT* treatment results in polycrystallization of the layer material (Fig. 5,*d*) for the I-type samples; in this case the granular structure was not detected. No marked changes of diffuse scattering with increased temperature were detected in the case of sample II.

The both sample kinds differ not only in respect of the pressure-induced defect structure changes but also indicate various roughness after the *HP–T* processing at 670 K under 1.1 GPa.

AFM images of the Ib sample subjected to the *HP–HT* treatments point to a creation of precipitates with mean height equal to about 1.5 nm (Fig. 6,*b*) or to surface roughness of about 3.4 nm for the case of Ia sample (Fig. 6,*c*). The surface of e sample II (Fig. 6,*d*) remains unchanged after the treatment and the same as in the untreated sample – 0.2 nm (AFM image of the as-grown Ib sample is presented in Fig. 6,*a*). This image is typical of all as-grown GaMnAs/GaAs samples.

The *HP–HT* treatment of the as-grown samples (as mentioned, practically no surface roughness has been detected for them) results in AFM – detectable visualization of defects.

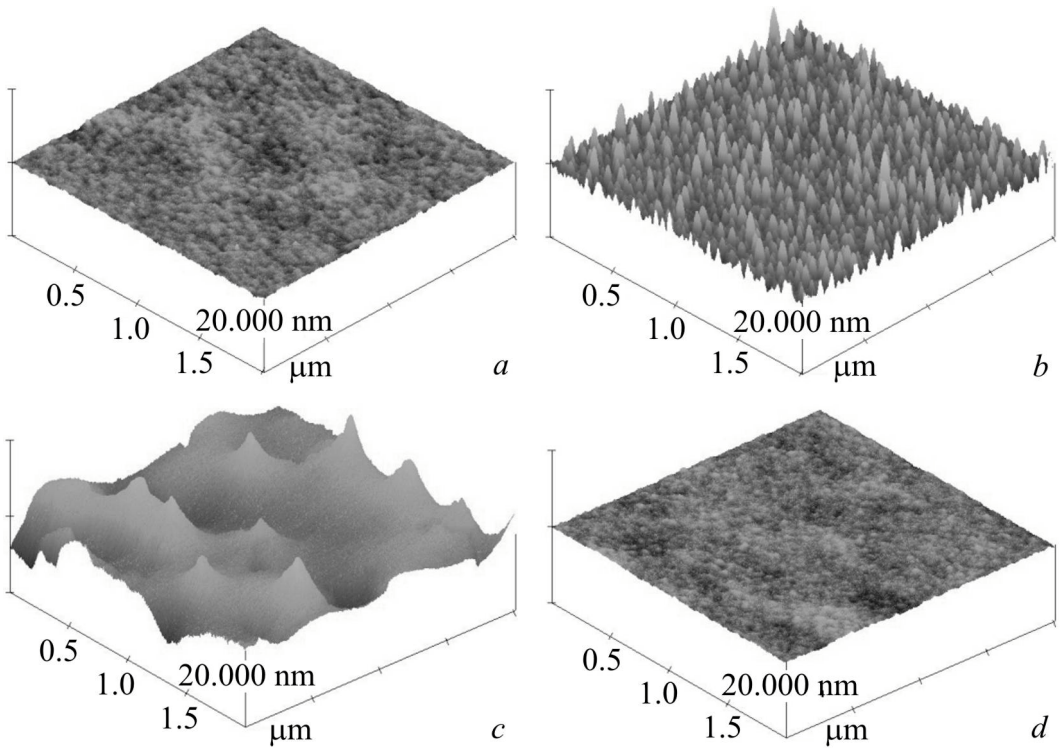

Fig. 6. AFM images of surface (2 × 2 μm area): *a*, *b* – sample Ib before and after *HP–HT* treatment, respectively; *c*, *d* – present AFM images for samples Ia and II, respectively, after *HP–HT* treatment

For the I-type samples, the post-growth treatment results in a reduced content of Mn interstitial defects. It is assumed that just Mn interstitials can segregate at the GaMnAs surface [9]. The role of As clusters, which can be also formed upon annealing, remains unclear and requires further studies. The changed surface roughness observed in the *HP–HT* treated GaMnAs samples is probably also related to the presence of various primary defects in the as-grown samples.

4. Conclusions

Annealing of Si:Mn results in crystallization of amorphous Si within the buried implantation–disturbed layer and in the formation of Mn_4Si_7 clusters. The influence of pressure-temperature conditions on a creations of the Mn_4Si_7 phase has been found.

Influence of annealing under enhanced hydrostatic pressure on the GaMnAs layer structure in GaMnAs/GaAs depends on numerous processing and material parameters, among them the annealing temperature and primary defects present in the as-grown layers. Enhanced pressure applied during annealing of the MBE-grown layers at 670 K results in increased strain in GaMnAs. The change of strain, from the compressive to tensile one, related to a creation of MnAs nanoclusters, is more pronounced after annealing under enhanced hydrostatic pressure. The high-pressure treatment at 920 K causes polycrystallisation of amorphous material or further increase of tensile strain in the samples, dependent also on the primary defect structure. No clear correlation between the Mn concentration and the changed GaMnAs lattice parameters (after the *HP–HT* treatment) was found.

This work was partially supported by the Ministry of Education and Science of Poland under the grant No. N20205232/1189.

1. *K.M. Bolduc, C. Awo-Affouda, A. Stollenwerk, M.B. Huang, F.G. Ramos, G. Agnello, V.P. LaBella*, Phys. Rev. **B71**, 033302 (2005).
2. *Shegqiang Zhou, K. Potzger, Gufei Zhang, A. Mucklich, F. Eichhorn, N. Schell, R. Grotzschel, B. Schmidt, W. Skorupa, M. Helm, J. Fassbender, D. Geiger*, Phys. Rev. **B75**, 0852003 (2007).
3. *M. Moreno, A. Trampert, B. Jenichen, L. Daweritz, K. Ploog*, J. Appl. Phys. **92**, 4672 (2002).
4. *M. Moreno, B. Jenichen, V.M. Kaganer, W. Braun, L.A. Trampert, L. Daweritz, K. Ploog*, Phys. Rev. **B67**, 235206 (2003).
5. *M. Moreno, V. Kaganer, B. Jenichen, L.A. Trampert, L. Daweritz, K. Ploog*, Phys. Rev. **B72**, 115206 (2005).
6. *M. Moreno, B. Jenichen, L. Daweritz, K. Ploog*, Appl. Phys. Lett. **86**, 161903 (2005).
7. *A. Misiuk, B. Surma, J. Bak-Misiuk*, Solid State Phen. **9**, 270 (2006).
8. *H. Park, K.S. Jones, J.A. Slinkman, M.E. Law*, J. Appl. Phys. **78**, 3664(1995).
9. *S.C. Erwin, A.G. Petukhov*, Phys. Rev. Lett. **89**, 227201 (2002).

J. Bak-Misiuk, P. Romanowski, J. Domagala, A. Misiuk, E. Dynowska, E. Lusakowska, A. Barcz, J. Sadowski, W. Caliebe

ФЕРОМАГНІТНІ НАНОКЛАСТЕРИ В Si:Mn І GaMnAs, ВІДПАЛЕНИХ ПРИ ВИСОКИХ ТЕМПЕРАТУРІ І ТИСКУ

Приведено результати вивчення дефектних структур шарів кремнію, імплантованого іонами Mn (Si:Mn) при різних температурах, і GaMnAs з подальшим відпалом при зовнішньому і високому тиску. Досліджено вплив умов відпалу на структурні властивості шарів Si:Mn і GaMnAs. Показано, що відпал імплантованих зразків Si:Mn призводить до кристалізації кремнію усередині заглибленого постімплантованого шару, а також до утворення феромагнітних Mn_4Si_7-виділень. Виявлено, що зміна в GaMnAs-шарі напруження з того, що стискає, на те, що розтягує, пов'язана з утворенням нанокластерів MnAs, залежить від умов обробки і початкових дефектів структури і не залежить від концентрації Mn. Обговорюється вплив первинних дефектів на структурні перетворення в шарі GaMnAs.